


RESEARCH

Open Access



Screening of dandelion phenolic extracts and their anti-bacterial function against *Escherichia coli* through acting on Na⁺-K⁺ ATPase

Pujun Xie^{1,2*}, Xiang Wang^{1,2†}, Lixin Huang^{1,2}, Yejun Deng^{1,2} and Caihong Zhang^{1,2}

Abstract

Food contamination by *Escherichia coli* (*E. coli*) is an increasing public health concern. Screening for natural plant preservatives has received increasing attention. In this study, dandelion flower phenolic extract (DFPE), with the strongest bacterial inhibition and the highest polyphenol level from various organs, was identified using HPLC and FTIR. The results showed a significant increase in extracellular ATP levels due to cellular membrane leakage in *E. coli* and decreased Na⁺-K⁺ ATPase activity. These behaviors were caused by representative phenolic compounds such as caffeic acid in DFPE. Molecular docking simulations were performed to reveal the mechanism of interaction between caffeic acid and Na⁺-K⁺ ATPase. This indicated that conventional hydrogen bonds, pi-anions, and pi-alkyl were involved in the interaction between them. Molecular dynamic equilibrium of the liganded ATPase complex was achieved after 20 ns. The lower values of Rg and SASA demonstrated that the liganded ATPase structure changed from a relatively loose to a tight state in the presence of caffeic acid. Overall, these findings are meaningful for screening bioactive compounds from various food-derived plant tissues using a combination of practical experimentation and molecular simulations.

Keywords Dandelion organs, Caffeic acid, Membrane leakage, ATPase inhibition, Molecular docking, Molecular dynamics simulation

[†]Pujun Xie and Xiang Wang contributed equally to this work.

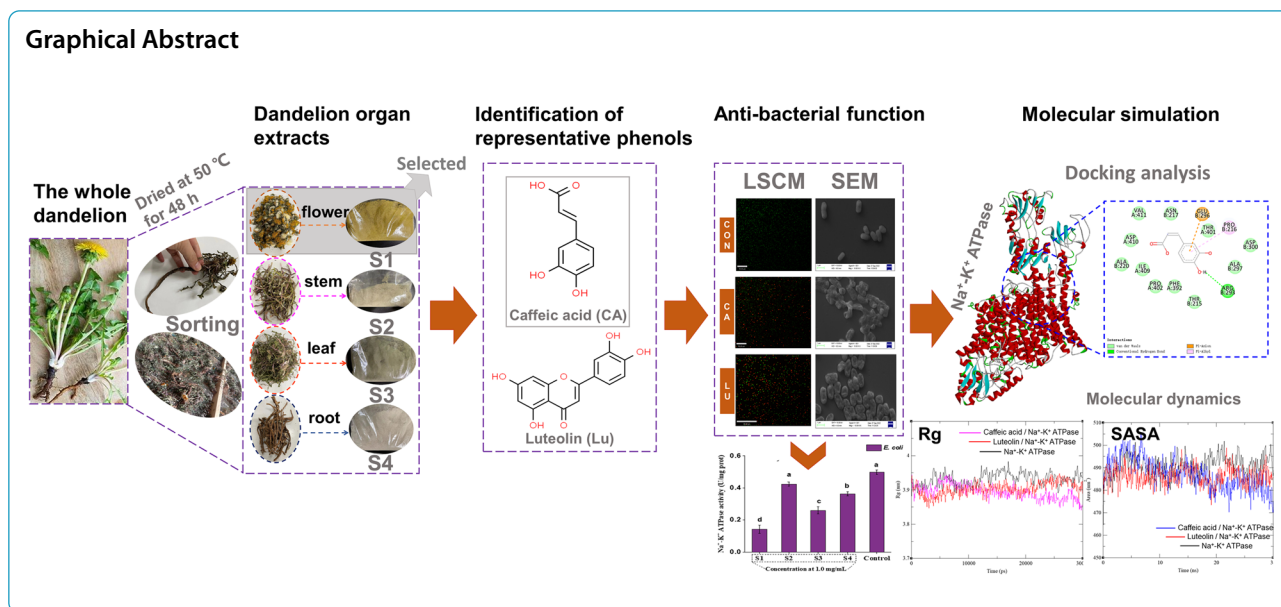
*Correspondence:

Pujun Xie

pujunxie@caf.ac.cn

Full list of author information is available at the end of the article





Introduction

Epidemiological studies have indicated that the leading pathogenic bacteria causing infectious diseases are principally *Escherichia coli* (*E. coli*), which is responsible for food contamination and health risks worldwide (Poolman & Anderson 2018). They can easily cause a wide variety of illnesses, including nausea, vomiting, stomach cramping, and diarrhea (Manges et al. 2019). Approximately 550 million people fall ill and 230,000 deaths are caused every year due to the consumption of contaminated food. Studies on the precautions for bacterial contamination have received a lot of attention. Currently, antibiotics from chemical synthesis are still used as effective antibacterial agents. However, increasing numbers of consumers are paying more attention to its potential side effects, such as initiating drug-resistant pathogens and destroying the gut microbiota. Screening a safe and effective natural antimicrobial product is one of the most promising ways against pathogenic microorganisms and is increasingly urgent.

Dandelion (*Taraxacum mongolicum* Weber ex F. H. Wigg.) belongs to the Asteraceae family with the Chinese name Pugongying (Hu 2018). As a medicinal and edible plant, thousands of dandelion species are found in the warmer temperature zones of the Northern Hemisphere worldwide, and about seventy species of them are rooted in China in terms of their taxonomy and morphology (Munoz et al. 2015). The medicinal use of *Taraxacum mongolicum* has been demonstrated for over one thousand years since the Tang dynasty (618–907 AD) in China. Currently, raw materials and extracts from the whole dandelion plant or its partial organs (e.g., roots,

leaves, stems, or flowers) are marketed as health-promoting products (Li et al. 2022). In particular, the whole or each part of the dandelion phenolic extract from different organs showed good antibacterial potential. For instance, flavonoids (luteolin and its glycosides) and phenolic acids (caffeic acid and chlorogenic acid) in dandelions display outstanding antimicrobial functions (Lopez-Garcia et al. 2013; Sengul et al. 2009). Dandelion root extract showed exceptional antimicrobial properties owing to the presence of vanillin and caffeic acid derivatives (Kenny et al. 2015). The whole dandelion extract, containing chlorogenic acid, luteolin, and caffeic acid, demonstrated bactericidal activity owing to its cellular membrane-breaking efficacy (Xu et al. 2021). Our previous results also implied that these phenols were enriched in dandelion leaves or stems (Xie et al. 2018). Similar phenolic compositions have also been found in dandelion flowers (Jedrejek et al. 2017). In addition, Na⁺-K⁺ ATPase, first discovered in 1957, is an electrogenic transmembrane ATPase that plays a key role in transporting ions across the plasma membrane of living cells (Kou 1957). This enables the transport of Na⁺ out and K⁺ into the cell, thereby maintaining their concentration gradients and electrolyte and fluid balance across the cell membrane (Xie & Askari et al. 2002; Fedosova et al. 2021). Therefore, Na⁺-K⁺ ATPase could potentially be used as an antibacterial target. Natural phenols with multiple hydroxyl groups, such as epigallocatechin-3-gallate, are excellent inhibitors of Na⁺-K⁺ ATPase (Ochiai et al. 2009). Nevertheless, to the best of our knowledge, comparative studies on the antibacterial effect of phenolic extracts from different dandelion organs (flowers, stems, leaves, and roots) are still

insufficient. In addition, further details related to the cell membrane $\text{Na}^+\text{-K}^+$ ATPase for their antibacterial mechanism are indistinct. Therefore, this study aimed to: (I) screen the key phenols with the best antibacterial efficacy of the extract from the flower, stem, leaf, and root of dandelion, as well as (II) uncover the anti-bacterial mechanism regarding the interaction of representative phenols from dandelion extract with $\text{Na}^+\text{-K}^+$ ATPase from the bacterial membrane. All findings will provide a discerning knowledge of the application of dandelion extracts as natural antimicrobial agents to achieve valorization. This study also highlights an effective strategy for screening bioactive compounds from plants.

Materials and methods

Raw materials, bacterial strain and chemicals

Fresh dandelions (*Taraxacum mongolicum*) were harvested during spring blooms from Shuyang County in eastern China. They were dried at 50 °C for 48 h until a constant weight was obtained, and then artificially detached into flowers, stems, leaves and roots. They were pulverized to a dry powder within 0.42 mm for subsequent use. The water used in this study was distilled in duplicate. Ethanol was purchased from Nanjing Chemical Reagents Inc. (Nanjing, China). Caffeic acid, luteolin, chlorogenic acid, *p*-coumaric acid, ferulic acid, rutin, quercetin, and luteolin-7-O-glycoside were purchased from Sigma-Aldrich, Inc. (St. Louis, MO, USA). *Escherichia coli* 1.4520 (*E. coli*) were purchased from China General Microbiological Culture Collection Center for assessment in vitro.

Strain activation of culture

The strains stored in glycerol tubes in MRS liquid medium at 4% (v/v) were inoculated and cultured in an incubator at 30 °C for 18–24 h. The streak plate method was used to select a single colony for purification and culture. The resulting strain was further cultured at 37 °C for 72 h and used as a working solution after subculturing for three generations.

Preparation of dandelion phenolic extracts

The dried dandelion organ powder (12.0 g) mixed with 75% ethanol–water (360 mL) was extracted for 30 min under ultrasound-assisted extraction at 25 °C and 720 W. Then, the extracted solution was obtained by vacuum filtration and evaporation at 55 °C for removing ethanol. The final dried powder of dandelion extracts was obtained by lyophilization for 48 h at -50 °C and 0.01 mbar by vacuum freezing drier device (VirTis Wizard 2.0, America).

Analysis and identification of phenolic compounds in dandelion extracts by HPLC and FT-IR

The phenolic compounds in various dandelion extracts derived from different organs (flower, stem, leaf and root) were quantified by an HPLC system (an automatic sampler, a binary pump and a vacuum degasser; Agilent Series 1260, Agilent Corporation, California, USA) coupled with a C_{18} analytical reversed column of Hypersil gold ODS2 (200 mm × 4.6 mm, i.d., 5 mm; Thermo Fisher, Waltham, MA, USA), which was executed at 30 °C according to the previous report (Xie et al. 2018). In detail, 2.0 mg/mL of dandelion extract powder dissolved in methanol was prepared for HPLC–UV–vis (Shimadzu Prominence LC-20A, Japan) equipped with a binary solvent manager and autosampler. The stationary phase was a C18 Hypersil gold ODS2 analytical column (250 × 4.6 mm i.d.) with a particle size of 5 mm (Thermo Fisher, USA), thermostated at 30 °C. The flow rate was 1.0 mL / min with 20 µL of injection level from samples, and the absorbance was detected at 280 nm. A linear gradient consisted of mobile phase B methanol and mobile phase A acetic acid (2%). The manipulated conditions for HPLC showed: keeping 5% B for 2 min; then a varied ranging from 5 to 20% for a duration of 10 min; a following varied ranging from 20 to 60% for a duration of 15 min; a further varied ranging from 60 to 70% for a duration of 5 min; lastly returning to initial status 5% B for a duration of 10 min. The phenolic compound content in the various dandelion samples identified in Table 2 was calculated using the peak area of their relevant standards. According to the previous protocol (Al-Hakkani 2019), the limit of detection (LOD) and the limit of quantification (LOQ) were obtained by the linearity of the calibration curve and its standard error as indicated in the following equations:

$$\text{LOD} = 3.3\sigma/S \quad (1)$$

$$\text{LOQ} = 10\sigma/S \quad (2)$$

where σ indicates a standard error and S indicates a slope of the linearity calibration curve.

ATR-FT-IR spectra of various dandelion samples were obtained using a Thermo Scientific Nicolet 6700 FT-IR spectrometer. ATR-FT-IR spectra were recorded in the range from 4000 to 500 cm^{-1} . The spectrometer parameters were set and a spectrum was obtained at a resolution of 4 cm^{-1} , 32 accumulated scans, and room temperature. The sample was shelved directly on the ATR crystal, pressed against the ATR crystal, and then scanned using the ATR-FT-IR spectrum. Thermo Electron's OMNIC software for FT-IR spectrometry was used to acquire the IR spectra.

Effect of dandelion phenolic extract on the inhibition of *E. coli*

The dandelion phenolic extracts (S1, flower; S2, stem; S3, leaf; and S4, root) at a mass ratio of 10% were added to MRS medium to obtain final concentrations of 0.05, 0.1, 0.5, and 1.0 mg / mL. The *E. coli* strain, with a 3% inoculation amount, was inoculated into the culture medium containing the extract. After culturing in a biochemical chamber at 30 °C for 24 h, the bacterial density OD600 was measured to evaluate the antibacterial effect of the extracts. Each sample was tested in triplicate. To further confirm the minimum inhibitory concentration (MIC) and minimum bactericidal concentration (MBC), the tested bacterial suspension (10^6 cfu / mL) was cultured with the dandelion extracts in the range of 0.05 to 1.0 mg / mL in broth at a shaking time of 48 h. The minimum concentration of dandelion extract that inhibits visible bacterial growth was defined as the MIC. Moreover, invisible bacterial growth in the tested sample was sub-cultured on nutrient agar, and the minimal concentration of dandelion extract that resulted in zero cfu / mL was defined as MBC.

Scanning electron microscopy analysis

The effect of dandelion flower phenolic extract (DFPE) on the cellular microstructure of *E. coli* was studied by scanning electron microscopy (SEM). The bacteria in the logarithmic growth phase used for the SEM test were first treated with DFPE (1.0 mg / mL for 24 h, and the test groups without DFPE for 24 h were used as controls. The treated bacterial suspension was centrifuged at $6000\times g$ for 8 min and the precipitated bacteria were washed with 0.05 M PBS (pH 7.20) and subsequently resuspended in 6.0 mL PBS (10^8 cfu / mL). The bacterial samples were installed on stainless steel and sprayed with a thin layer of gold (Au), and their microstructures were observed using SEM (Zeiss EVO LS10, Carl Zeiss NTS, Oberkochen, Germany) at an accelerating voltage of 20 kV.

Measurement of leakage intracellular ingredients

Intracellular ingredient release was measured using prior protocols (Wang et al. 2022; Zhao et al. 2015). Nucleic acid loss was determined using a microplate reader (MD iX3, MA, USA) at 260 nm. Dandelion extracts (S1, flower; S2, stem; S3, leaf; and S4, root) at a concentration of 1.0 mg / mL were added to test tubes containing *E. coli*, and the resulting bacteria were cultivated at 37 °C for 3 h. The bacterial suspension was centrifuged at $6000\times g$ for 8 min, and the supernatant was collected. After micro-filtration through the filter membrane, the absorbance at 260 nm was recorded. The sample in the test tube without the dandelion extract was used as a control.

Laser Scanning Confocal Microscopy (LSCM) analysis

E. coli cells assayed in the logarithmic phase were selected to study the permeability changes in the cellular membrane treated with DFPE. They were assessed by LIVE/DEAD viability assay using confocal laser scanning microscopy (CLSM). Briefly, bacterial cells were suspended in 0.85% NaCl buffer to a concentration of approximately 10^8 cfu / mL. 0.1 mL DFPE / caffeic acid / luteolin solution at MIC were blended with 1.0 mL bacterial suspensions. After 4 h of incubation, the bacterial cells were obtained by centrifugation at $4500\times g$ for 9 min at 4 °C, resuspended in 0.85% NaCl buffer, and dyed using the fluorescent probes of the viability kit (BBcellProbe[®] N01/PI) as stated in the instructions. The probe-treated cells were monitored using LSCM (Perkin Elmer, Waltham, Mass, USA) with laser light at 480 nm.

Detection of extracellular ATP level

The ATP level in *E. coli* treated with dandelion extracts (S1, flower; S2, stem; S3, leaf; and S4, root) was measured using an ATP assay kit (Jiancheng Bioengineering Institute, Nanjing, China). First, strain samples of *E. coli* were prepared. The bacterial suspension was separated into different test tubes, and added with 1.0 mg / mL of dandelion phenolic extracts, respectively. Subsequently, each test group was cultured at 37 °C for 4 h and then centrifuged at $3000\times g$ for 5 min to obtain a bacterial pellet. These bacterial samples were washed twice with phosphate buffered saline (PBS), resuspended in 0.5 mL muramidase (10 g / L) and 0.5 mL Tris-EDTA buffer solution (5.0 mM Tris-HCl, 0.5 mM EDTA, pH 8.0), and incubated at 37 °C for 20 min. The resulting samples were diluted with PBS (5.0 mL), placed in an ice bath for 6 min, and then centrifuged. The supernatant was then collected for further testing. A bacterial suspension without dandelion extract served as a control.

Detection of cellular Na⁺-K⁺ adenosine triphosphatase (Na⁺-K⁺ ATPase) activity assay

The Na⁺-K⁺ ATP enzyme is present in the membranes of cells and organelles. It is a protease on biofilms and plays an important role in cellular volume regulation, material transport, energy conversion, and information transmission. Enzyme activity undergoes a series of changes when the breaking cell is related to enzyme activity. The assay principle is that ATPase decomposes ATP to generate ADP and inorganic phosphorus. Therefore, ATPase activity can be determined by the amount of inorganic phosphorus. One unit (1 U) of ATPase activity is defined as the amount of ATPase in one milliliter cell homogenization solution can produce 1.0 μmol inorganic phosphorus per hour.

The inhibition of ATPase by dandelion extracts (S1, flower; S2, stem; S3, leaf; and S4, root) from *E. coli* was measured using an ATPase assay kit (Jiancheng Bioengineering Institute, Nanjing, China). The absorbance of the treated bacterial cells at 636 nm was measured using an ultraviolet spectrophotometer (SPECORD 210, Analytik Jena, Germany) according to the kit instructions.

Molecular docking analysis

Na⁺-K⁺ ATPase is widely distributed in the membrane of *E. coli* and facilitates the maintenance of the resting potential, availability of transport, and cellular morphology. To study the inhibitory mechanism in *E. coli*, the key phenolic compounds docked with Na⁺-K⁺ ATPase from its membrane proteins were investigated. The protein structure (PDB ID: 7nnl) of *E. coli* was obtained from the RCSB Protein Data Bank (<http://www.rcsb.org>) and was marked as a protein receptor. The water in the protein was removed and hydrogen atoms were added before executing the docking procedure. After energy minimization for structural optimization, the key representative phenolic compounds in the dandelion extract were successfully docked with the treated protein using Autodock Tools 1.5.7, and their docking interactions in a two-dimensional diagram were displayed using Accelrys Discovery Studio v 4.0.

Molecular Dynamics (MD) simulation

To further investigate the intention of the primary binding mode confirmation and to obtain an overall impression of the caffeic acid and luteolin represented from dandelion extracts in the binding site of Na⁺-K⁺ ATPase from *E. coli*, a molecular dynamics simulation was implemented with some modifications according to a previous protocol (Lu et al. 2022). The lowest docking energy was selected as the initial conformation for MD analysis.

Specifically, MD simulations were executed using the GROMACS (v. 2022.2) software package with the Amber99sb-ildn force field. A periodic cubic box was used to fix the phenol-ATPase complexes, in which a TIP3P water model was inserted for solvation. To neutralize the protein charge, an appropriate quantity of Na⁺ was added. Next, the resulting energy-minimization simulation was performed. The Particle Mesh Ewald model was employed to assess long-range interactions. A 10 Å cut-off was used to treat the van der Waals interactions. All the hydrogen-associated bonds were constrained using the LINCS algorithm. The temperature and pressure couplings were conducted using a V-rescale thermostat and Parrinello-Rahman barostat, respectively. The NVT and NPT ensembles were also used to create the systems for 100 ps. Consequently, a simulation period of 30 ns was used.

Statistics

All assays were performed in triplicate, and the data are presented as mean values ± relative standard deviation (RSD). Statistically significant differences between two parameters were determined by one-way analysis of variance (ANOVA) the Origin 7.0 (OriginLab Co. LTD, MA, America). Further data analysis, followed by Fisher's Least Significant Difference (LSD) test, was performed. The findings with different letters (a-h) in the upper right corner are considered significantly different at $p < 0.05$.

Results and discussion

Identification and characterization of dandelion phenolic extracts from different organs

The phenolic compounds extracted from various dandelion organs (flowers, stems, leaves, and roots) using HPLC were identified, as shown in Fig. 1. It was observed that the level of phenolic compounds containing both flavonoids and phenolic acids varied depending on the specific dandelion organ. For instance, the lowest level at 38.36 mg / g of total phenolic compounds was observed in dandelion root extract. The highest level at 240.25 mg/g of total phenolic compounds was observed in the dandelion flower extract. This result was 6.3-fold higher than that from dandelion root extract, 2.4-fold higher than that from dandelion stem extract, and 1.64-fold higher than that from the dandelion leaf extract. Among them, the level of total phenolic acid was dominant in the leaf extract, and the level of total flavonoids was dominant in the stem extract. Both total phenolic acid and flavonoid levels were enriched in the flower extract, whereas other types of phenols were inadequate. Moreover, the detailed results in Table 1 showed that these phenolic acids (caffeic acid, ferulic acid, and chlorogenic acid) and flavonoids (luteolin, quercetin, and luteolin-7-O-glycoside) were present in dandelion flower (Table 1A), stem (Table 1B), leaf (Table 1C), and root (Table 1D) extracts. Specifically, as Table 2 indicated, the flower extract was substantially composed of caffeic acid (118.27 mg / g) and luteolin (82.93 mg / g). The total level of these phenolic compounds was 84% of all the identified phenols. The leaf extract was rich in caffeic acid (106.20 mg / g). The stem extract was rich in luteolin (70.02 mg / g), whereas other phenols, such as organic acids, were insufficient. The phenolic extract of dandelion stem mainly contained luteolin, and a small quantity of organic acids, such as caffeic acid; the content was only 5.89 mg / g. Compared with other tissue extracts, the phenolic extract of the dandelion stem also contained rutin, approximately 6.75 mg / g. In terms of the phenolic extract, the main components in dandelion leaves were very similar to those in dandelion flowers, but the content of luteolin was significantly lower, reaching only

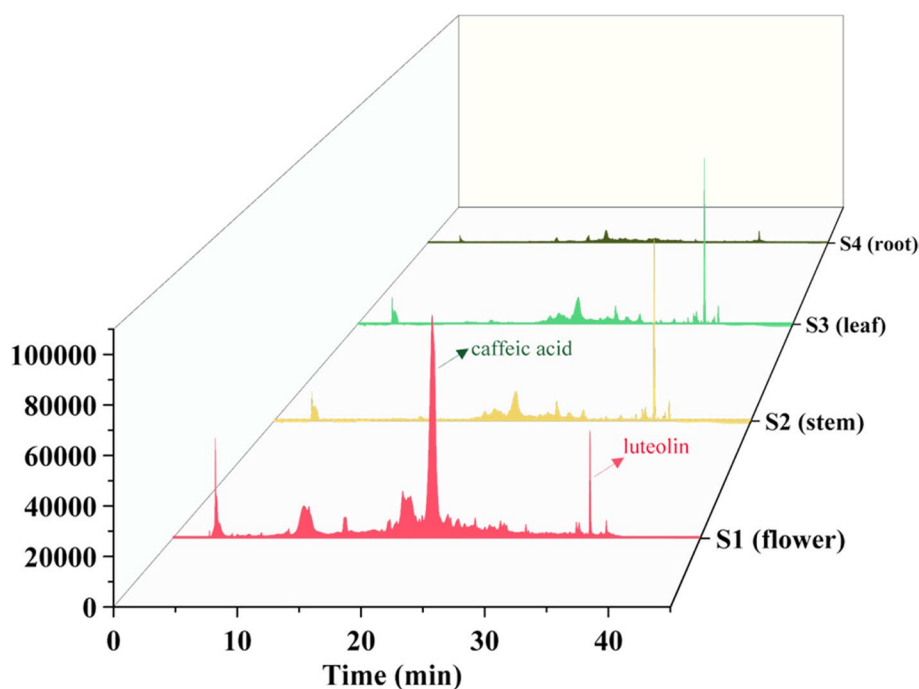


Fig. 1 HPLC of phenolic compounds in dandelion extracts from flower, stem, leaf and root

10.09 mg / g. The phenolic extract of the dandelion root had the lowest phenol content compared with the other tissue extracts. It also mainly contained caffeic acid and quercetin, with the contents of 17.95 mg / g and 9.52 mg / g, respectively. The lowest total phenol content was derived from the dandelion flower extract, 240.25 mg / g and 97.69 mg / g, respectively; The lowest total phenol content was derived from dandelion root extract, which was 38.36 mg / g. In summary, the dandelion phenolic extracts were mainly composed of caffeic acid and luteolin, among which the dandelion flower phenolic extract reached the highest level. The significant difference in phenolic compounds distributed in different plant organs was due to photosynthesis intensity and genotypes (Kolton et al. 2022; Minutolo et al. 2013). Therefore, these phenolic compounds were concentrated in the dandelion flowers and leaves.

FT-IR of dandelion extracts

The basic chemical structural characteristics of the phenolic compounds in the dandelion extracts were determined by Fourier Transform infrared spectroscopy (FT-IR). Figure 2 showed the infrared spectra of the dandelion phenolic extracts. All the dandelion phenolic extracts (S1-S4) had a strong absorption peak at 3250 cm^{-1} , which was due to the stretching vibration caused by caffeic acid and O-H in quercetin and was an intermolecular hydrogen bond. There was a weak

absorption peak at 2925 cm^{-1} , which corresponded to the vibrational stretching peak of the C-H bond on the benzene ring of polyphenols (i.e., caffeic acid and luteolin). The wavenumbers of the C=C asymmetric stretching vibrational absorption peak in polyphenols (i.e., caffeic acid and luteolin) ranged from 1601 cm^{-1} to 1612 cm^{-1} . The wavenumbers of the C-O stretching vibration absorption peaks of polyphenol compounds (i.e., caffeic acid and luteolin) were 1046 cm^{-1} and 1037 cm^{-1} , respectively. The O-H in-plane bending vibrations of polyphenolic compounds (i.e., caffeic acid and luteolin) were 1380 cm^{-1} and 1371 cm^{-1} , respectively. These results are in good agreement with previously reported findings (Di Pasqua et al. 2006).

Anti-bacterial assessment of various dandelion organ extracts against *E. coli* in vitro

Figure 3 showed the inhibitory effects of polyphenol extracts from different dandelion organs (flowers, stems, leaves, and roots) on *E. coli*. As indicated in Fig. 3, the dandelion flower phenolic extract had the strongest inhibition against *E. coli*, with an IC₅₀ of approximately 0.5 mg / mL, followed by the dandelion leaf phenolic extract, which showed an inhibitory rate against *E. coli* reaching 68.0% at a concentration of 1.0 mg / mL. Both stem and root extracts showed negligible inhibiting power, and their inhibitory rate was less than 30.0% at a concentration of 1.0 mg / mL.

Table 1 HPLC-TOF-MS/MS of phenolic extracts from different organ dandelions; Sample A (dandelion flower phenolic extract), Sample B (dandelion stem phenolic extract), Sample C (dandelion leaf phenolic extract), Sample D (dandelion root phenolic extract)

Samples	Compounds	Centroid mass (Da)[M-H]	Intensity ($\times 10^3$)	Time (min)	Fragments, m/z
A	caffeic acid	179	266	14.97	179.1, 134.9, 107.2
	apigenin	269	59.3	31.35	269.3, 251.4, 201.5, 168.9, 117.2, 106.9
	luteolin	285	2090	20.53	285.1, 241.2, 199.1, 175.1, 133.1
	isoetin	293	372	27.95	293.2, 275.3, 235.3, 231.6, 191.6
	quercetin	301	5.1	28.18	301.1, 164.9, 175.3, 136.8, 121.1
	chlorogenic acid	353	21.6	12.61	352.9, 191.3, 178.9, 135.1, 127.2
	luteolin-7-O-glycoside	447	90.7	18.63	446.9, 284.9, 199.1, 175.3
	B	caffeic acid	179	40.7	14.88
ferulic acid		193	9.02	13.37	193.1, 175.6, 165.3
apigenin		269	5.56	21.95	268.9, 224.9, 200.9, 117.1
luteolin		285	162	20.67	285.1, 241.1, 199.1, 175.1, 133.1
isoetin		293	157	27.42	293.2, 275.2, 235.2, 223.2, 195.4
quercetin		301	13.0	26.72	301.2, 273.1, 257.4, 164.9, 121.2
chlorogenic acid		353	11.4	16.90	352.9, 191.3, 178.9, 135.2
luteolin-7-O-glycoside		447	10.7	17.97	446.9, 400.8, 331.6, 295.1, 161.2, 133.1, 106.9
C	<i>p</i> -coumaric acid	139	12.5	32.61	157, 139, 110.9, 94.8, 70.7
	caffeic acid	179	275	14.99	179.2, 135.1, 107.3
	ferulic acid	193	9.48	22.48	193.1, 177.1, 149.3
	apigenin	269	55.4	31.37	269.2, 201.1, 172.9, 156.8
	luteolin	285	658	20.71	285.0, 217.1, 199.1, 175.1, 133.1
	isoetin	293	89.9	30.93	293.2, 275.2, 231.2, 183.1, 171.1
	quercetin	301	6.83	28.12	301.1, 233, 164.9, 120.8
	chlorogenic acid	353	33.8	16.84	353.2, 191.3, 179.1, 135.2
D	luteolin-7-O-glycoside	447	33.7	22.94	447.9, 429.6, 327.1, 311.2
	cichoric acid	473	44.9	15.37	472.9, 310.9, 292.9, 265.1, 178.9, 112.9
	luteolin-7-O-glycoside	447	16.1	17.97	446.9, 295.1, 160.9, 106.8
	chlorogenic acid	353	168	28.59	353.2, 177.1, 163.1
	quercetin	301	11.6	26.73	301.1, 173.3, 165.2
	Isoetin	293	70.0	24.04	293, 236, 221, 205.1, 177.1, 148.1
	luteolin	285	43.9	20.71	285, 217.1, 175.1, 133.1
	apigenin	269	27.2	31.35	269.2, 201
ferulic acid	193	13.4	22.52	193.1, 148.9, 104.9	
caffeic acid	179	76.8	15.03	178.9, 135	

Dandelion phenolic flower and leaf extracts were rich in caffeic acid and luteolin, as mentioned above. These polyphenols can combine with the divalent cations of the bacterial outer membrane, resulting in bubbles, depression, and collapse of the cell wall, as well as the integrity of the cell wall. At the same time, plant polyphenols were found to change the composition of fatty acids in the cell membrane and inhibit the synthesis of ergosterol, thereby reducing the fluidity of the cell membrane and improving its permeability of cell membrane (Pinto et al. 2009; Wongsa et al. 2022). Therefore, caffeic acid or luteolin are very likely to change the permeability of the cell membrane to cause intracellular ATP leakage or to interact

with ATPase, and then affect the energy metabolism of microorganisms to inhibit bacteria. This deduction was confirmed by further investigation of the inhibitory mechanisms of caffeic acid and luteolin against *E. coli*.

Effect of dandelion flower phenolic extract on the cellular membrane of *E. coli*

The cell death levels of *E. coli* were investigated, as shown in Fig. 4a–d. Untreated *E. coli* cells presented clearly visible and uniform green fluorescence, indicating that the cells in the control group exhibited normal physiological activity. The fluorescence signal in the bacterial cells exposed to dandelion flower phenolic extract (DFPE) at

Table 2 Quantification of phenolic compounds in dandelion extract from different organs by HPLC–UV–Vis

Phenolic compounds	R.T. (min)	Standard curve	R ²	LOD [†] (ng/mL)	LOQ [‡] (ng/mL)	Content (mg/g)			
						Flower	Stem	Leaf	Root
chlorogenic acid	18.3	Y=0.16 X+7.83	0.998	0.51	1.55	1.87±0.03 ^c	—	14.23±0.03 ^c	5.80±0.28 ^b
caffeic acid	22.6	Y=0.07 X+12.61	0.997	3.03	9.18	118.27±1.2 ^a	5.89±0.3 ^d	106.2±3.7 ^b	17.95±0.1 ^c
cichoric acid	25.4	Y=6.13 X+2.07	0.992	0.12	0.36	—	—	—	0.16±0.03
p-coumaric acid	26.1	Y=0.36 X+4.28	0.999	0.22	0.67	—	—	12.76±0.95 ^a	—
ferulic acid	27.3	Y=0.11 X+6.04	0.998	1.31	3.97	9.66±0.57 ^a	0.26±0.01 ^c	3.22±0.24 ^b	—
isoetin	28.9	Y=5.34 X+1.51	0.995	0.39	1.18	0.53±0.012 ^a	0.029±0.005 ^c	0.37±0.031 ^b	0.015±0.004 ^c
rutin	32.7	Y=0.28 X+4.78	0.999	0.63	1.91	—	6.75±0.22	—	—
luteolin	35.3	Y=0.19 X+9.67	0.997	0.86	2.61	82.93±3.1 ^a	70.02±1.5 ^b	10.09±0.7 ^c	—
apigenin	36.1	Y=2.67 X+12.90	0.998	0.15	0.45	0.18±0.03 ^a	0.09±0.001 ^b	0.16±0.02 ^a	0.02±0.003 ^c
quercetin	37.4	Y=0.92 X+2.95	0.996	2.57	7.79	9.51±0.61 ^a	7.13±0.69 ^b	2.34±0.69 ^c	9.52±0.72 ^a
luteolin-7-O-glycoside	37.6	Y=0.19 X+8.32	0.999	0.11	0.33	5.25±0.38 ^b	7.96±0.47 ^a	4.38±0.33 ^b	5.09±0.26 ^b
Total flavonoids	—	—	—	—	—	96.28±1.8 ^a	75.07±3.2 ^c	88.69±0.9 ^b	6.08±0.5 ^d
Total phenolics	—	—	—	—	—	240.25±5.0 ^a	97.69±1.9 ^c	123.1±2.1 ^b	38.36±1.2 ^d

Letters (a-d) indicate significantly different values at $p < 0.05$ as measured by Fisher LSD's test. The content of the phenolic compounds in different dandelion tissues was measured by HPLC protocol mentioned 2.4. based on its the peak area of the corresponding phenolic standards. Total flavonoid and total phenol content of dandelion extracts for each organ sample was measured by plant flavonoids test kit and plant total phenol test kit from Nanjing Jiancheng Bioengineering Institute (<http://www.njjcbio.com/>). Besides, for the standard curve of phenolic compounds, Y indicates a peak area related to X sample concentration ranging from 0.1 to 10 mg/mL

R.T. indicates retention time

[†] LOD indicates limit of detection (S/N=3)

[‡] LOQ indicates limit of quantitation (S/N= 10). S/N represents a signal-to-noise rate. LOD and LOQ were obtained by the linearity of the calibration curve and its standard error as indicated in the following equations: $LOD = 3.3\sigma / S$; $LOQ = 10\sigma / S$, where σ indicates a standard error and S indicates a slope of the linearity calibration curve

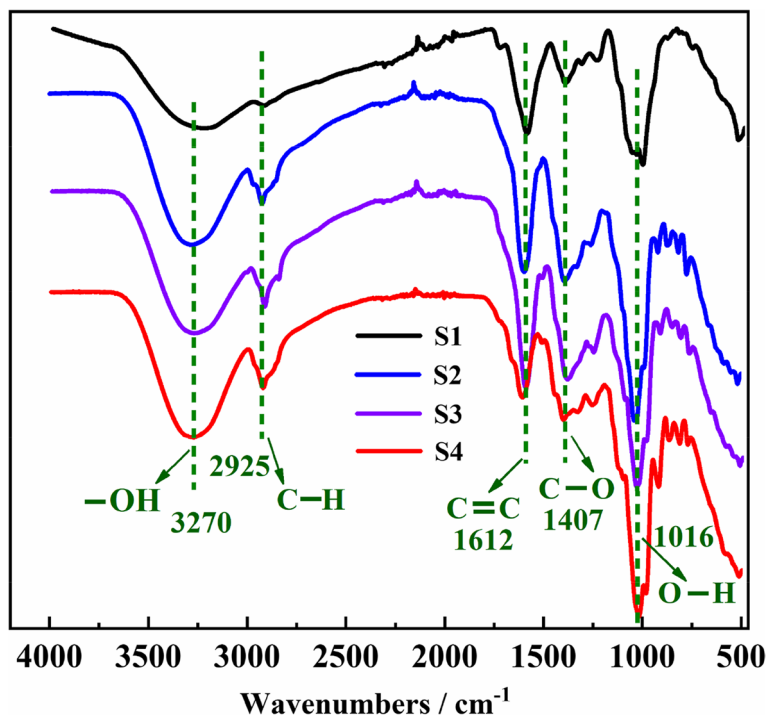


Fig. 2 FT-IR of various dandelion extracts: S1, flower; S2, stem; S3, leaf; and S4, root

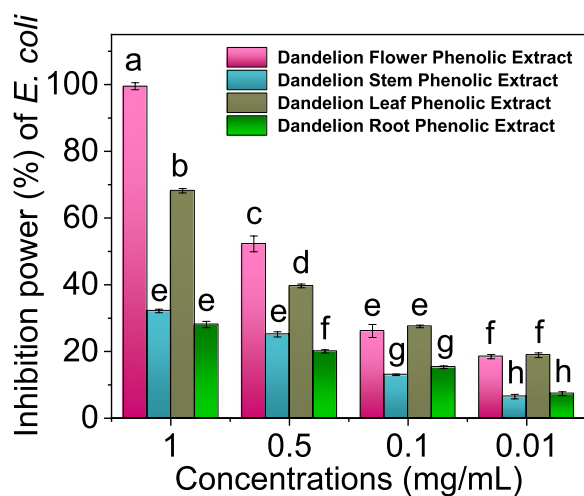


Fig. 3 Dandelion flower phenolic extract (pink), dandelion stem phenolic extract (blue), dandelion leaf phenolic extract (brown), dandelion root phenolic extract (green). Letters (a-h) indicate significantly different values at $p < 0.05$ as measured by Fisher LSD's test

MIC gradually shifted from green to red. Green fluorescence decreased significantly, suggesting the reinforcement of membrane permeability in the treated groups. When DFPE, including caffeic acid and luteolin, at an MBC concentration of 1.0 mg / mL was added to the bacterial medium, *E. coli* cells emitted strong red fluorescence and the green fluorescence became almost invisible. This indicated that these bacteria were severely damaged. As shown in Fig. 4e, the morphology of the *E. coli* cells was regular, plump, and smooth in an intact form. After 6 h of treatment with 1.0 mg / mL DFPE, caffeic acid, or luteolin, the cell surface became bumpy, coarse, and damaged to some degree. As observed in Fig. 4f, g, and h, the cells severely collapsed and the membrane of the treated cell was more intensively damaged, which demonstrated that leakage of the cell cytoplasm was induced. DFPE, including its representative phenolic compounds (caffeic acid and luteolin), was accessible to the cell surface of *E. coli*, resulting in permeability of the bacterial wall and even death. As such, DFPE, including caffeic acid and luteolin, constantly penetrates the bacterial membrane to disturb its normal physiological metabolism, thereby inactivating bacterial cells (Morones et al. 2005).

Disruption of the outer membrane plays a key role in the antibacterial activity of DFPE against *E. coli* (Zhou et al. 2020). $\text{Na}^+ - \text{K}^+$ -ATPase is a pivotal carrier protein embedded between the phospholipid bilayer of the cell membrane that controls the transmembrane transport of Na^+ and K^+ . As indicated in Fig. 4i, j, and k, the $\text{Na}^+ - \text{K}^+$ -ATPase activity of *E. coli* treated with DFPE significantly decreased. In addition, intracellular ATP concentrations significantly decreased due to increased concentrations of extracellular ATP. Because ATP is a well-polarized compound that cannot be released in normal cells, this observation of DFPE-induced cell membrane induced by DFPE was confirmed to be reasonably explained as well. These findings were derived from depolarized cells, altered cell morphology, and consequent damage to the cell membrane (Guo et al. 2019). Among the dandelion organ extracts, DFPE (S1) showed the strongest inhibition of $\text{Na}^+ - \text{K}^+$ -ATPase activity. The decreased activity of $\text{Na}^+ - \text{K}^+$ -ATPase compared with the control is shown in Fig. 4j, indicating that damage to the integrity of the cellular membrane occurred in *E. coli* treated with DFPE. Additionally, extracellular ATP concentrations were measured (Fig. 4k). The results showed that extracellular ATP concentrations increased significantly when stained cells were treated with DFPE (S1). Similar observations were made for dandelion leaf phenolic extract (S2). This may be due to the similar levels of phenolic compounds (caffeic acid and luteolin) in the extracts. For DFPE (S1), the extracellular ATP concentrations for *E. coli* were notably increased ranging from 5.11 $\mu\text{mol} / \text{L}$ to 6.69 $\mu\text{mol} / \text{L}$ after 3 h. The similar trend of dandelion leaf phenolic extract (S2) to DFPE (S1) performance can be observed as well. The higher intracellular ATP concentrations were derived from the inhibition of ATPase related to this work, which leaked from the cell inside to the outside. All of these joint actions forced *E. coli* cell apoptosis. In addition, the great alteration of ATP levels inside and outside the bacterial cell membrane resulted in an unregulated disorder, eventually leading to the destruction of the integrity of the cytoplasmic membrane and causing the bacteria to induce apoptosis (Augustin et al. 2006). Therefore, DFPE (S1) inhibits the proliferation of *E. coli* by lowering the activity of $\text{Na}^+ - \text{K}^+$ -ATPase.

(See figure on next page.)

Fig. 4 Effect of dandelion flower phenolic extract (DFPE) on nucleic acid of *E. coli*; CLSM images of *E. coli* treated by samples (a control; b DFPE; c caffeic acid; d luteolin); SEM images of *E. coli* treated by samples (e control; f DFPE; g caffeic acid; h luteolin); Anti-bacterial biological characterization (i $\text{OD}_{260\text{nm}}$; j $\text{Na}^+ - \text{K}^+$ ATPase activity; k extracellular ATP level): S1, DFPE; S2, dandelion stem phenolic extract; S3, dandelion leaf phenolic extract and S4, dandelion root phenolic extract. Letters (a-d) indicate significantly different values at $p < 0.05$ as measured by Fisher LSD's test

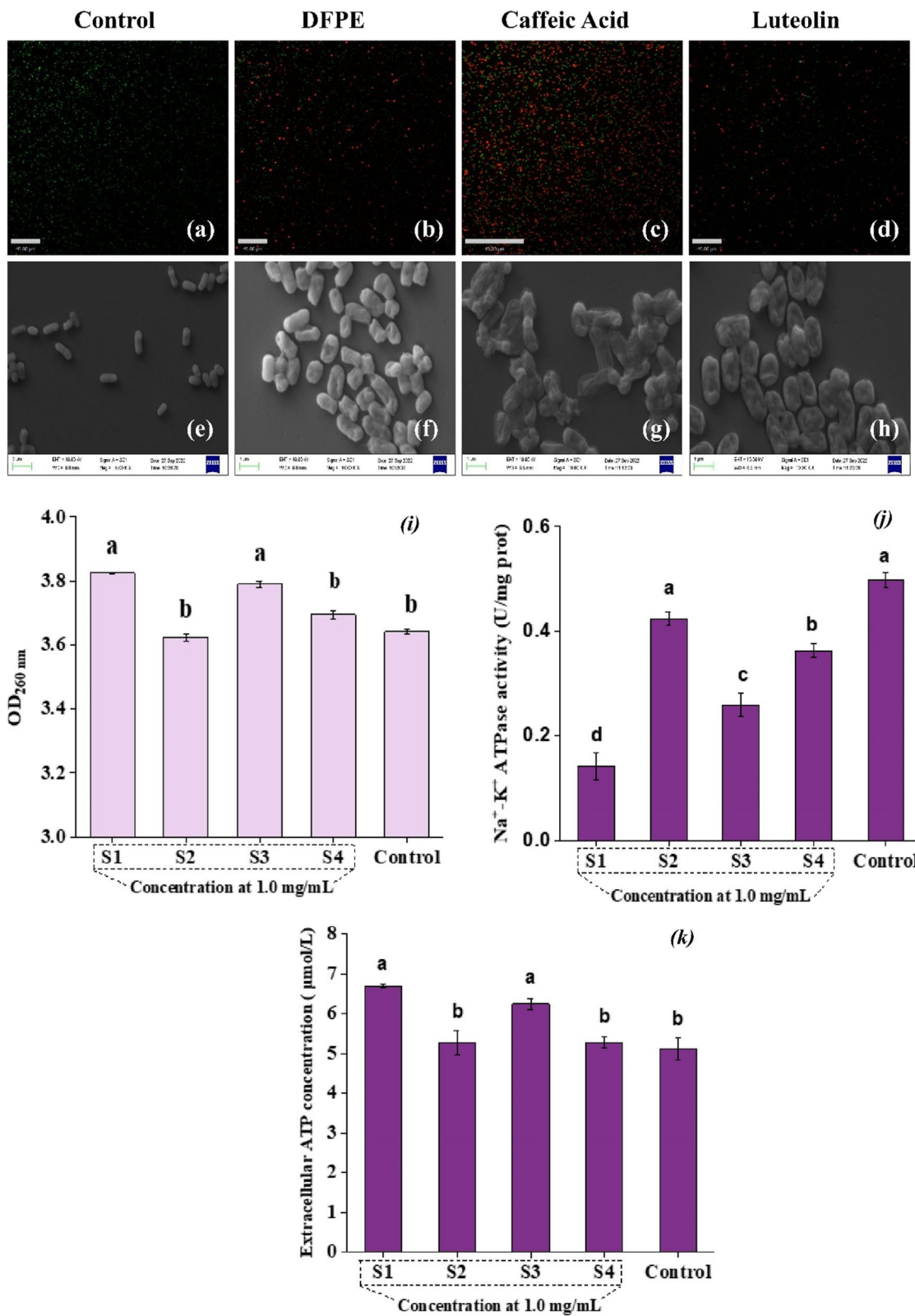


Fig. 4 (See legend on previous page.)

Docking analysis between the representative phenols in dandelion extracts and the ATPase in the bacterial membrane

The cellular membrane of bacteria, composed of proteins and lipids, is a multifaceted tissue that can envelop cell cytoplasm and plays a crucial role in maintaining cytoskeleton shape and protecting the integrity of the interior of the cell for viability. To discover potential cell-permeable inhibitors from dandelion flower phenolic extract (DFPE) and explore the mechanism of cell breakage, Na⁺-K⁺ ATPase was selected as a receptor for docking with key phenols in DFPE because it is a vital and prevailing target for chemotherapeutic treatment of bacterial infections. The representative phenols (caffeic acid and luteolin) in DFPE were docked with ATPase. As observed in Fig. 5a, b, either caffeic acid or luteolin can effectively dock with ATPase, suggesting van der Waals, Pi-donor hydrogen bonds, and conventional hydrogen bonds. Specifically, the H or O atom in the hydroxyl (C4) and carbonyl groups of caffeic acid enables docking with O or H in the amino acid residue of the ATPase receptor. The carbon hydrogen bond resulting from atom O (C7) in luteolin with atom H in amino acid (LEU, No.530) and van der Waals force resulting from luteolin and 16 amino acids were formed from docking with the ATPase of *E. coli*. These interactions possibly contributed to the inhibition of ATPase activity and affected the membrane physiological properties and multifaceted functions, such as membrane potential, depolarization, and fluidity, which led to the damage of the cell membrane to release intracellular cytoplasm. Moreover, the best affinity for caffeic acid and luteolin binding with the ATPase of *E. coli* reached -8.1 kcal / mol and -6.4 kcal / mol, respectively. It was noted that caffeic acid seemed to inhibit ATPase better than luteolin due to its lower binding energy. These results were in good agreement with previously reported findings (Dai et al., 2021; Qi et al. 2022). Moreover, Na⁺-K⁺ ATPase, as a transmembrane protein, facilitates the active transport of three Na⁺ ions out of the cell and two K⁺ ions into the cell at the expense of ATP. It can stabilize ionic homeostasis and maintain membrane potential. Na⁺-K⁺ ATPase consists of α and β subunits. The α -subunit of Na⁺-K⁺ ATPase has catalytic activity for the enzyme with binding sites for cardiac glycosides, ions, and ATP. The β -subunit is inserted into the membrane to facilitate cell adhesion, cell volume, and signal transduction (Chakraborti et al. 2016). These physiological processes are crucial to bacterial growth. When the α -subunit of Na⁺-K⁺ ATPase interacts with caffeic acid and luteolin in DFPE, this behavior can result in a decreased membrane potential, a smaller cell volume, and cellular signal disorder

(Pivovarov et al. 2018). Therefore, strong inhibition of the growth of *E. coli* treated with DFPE was observed.

Molecular Dynamics (MD) analysis

Figure 6 showed some vital parameters, such as root mean square deviation (RMSD, (A)), root mean square fluctuation (RMSE, (B)), radius of gyration (Rg, (C)), solvent accessible surface area (SASA, (D)), and hydrogen numbers (E)) between key representative phenols (caffeic acid / luteolin) and Na⁺-K⁺ ATPase (receptor protein) in the process of MD. Generally, a steady state of dynamic equilibrium could be reached when the fluctuation of RMSD was kept reasonably constant within a 0.1 nm range (Shi et al. 2021). As shown in Fig. 6, Na⁺-K⁺ ATPase activity resulting from caffeic acid and luteolin exhibited different behaviors compared to the protein itself. Overall, a small fluctuation of rise emerged in their complex due to the irregular motion of atoms induced by temperature and water molecules present in the MD environment, as indicated in Fig. 6A. Nevertheless, a significant increase was observed in caffeic acid / ATPase and luteolin / ATPase before 20 ns. Equilibrium is achieved after 20 ns. This is because either caffeic acid or luteolin can interact with the Na⁺-K⁺ ATPase and then change its structure to become tighter and more compact compared to the protein itself. As caffeic acid or luteolin penetrated Na⁺-K⁺ ATPase, the protein probably adjusted its structural conformation and expanded first when binding caffeic acid or luteolin. In addition, caffeic acid showed a lower RMSD value than luteolin (Fig. 6A), implying stronger binding to the protein resulting from caffeic acid. Thus, the lower RMSD values of the liganded protein revealed the stability of the protein and its favorable binding during the entire simulation period.

RMSF plots against the residual numbers of Na⁺-K⁺ ATPase with caffeic acid or luteolin are shown in Fig. 6B. In contrast to the native protein, the structural flexibility of amino acids in Na⁺-K⁺ ATPase interacting with caffeic acid or luteolin was dramatically decreased, indicating that the interaction between these phenols and protein not only restricted the movement of the phenols but also stabilized the amino acid flexibility of the hydrophobic pocket. In contrast, the residues of the protein located in the luteolin binding site were more rigid owing to the instability of the complexes. This resulted in binding to the hydrophobic surface instead of the hydrophobic pocket.

Plotting Rg for Na⁺-K⁺ ATPase with caffeic acid or luteolin was related to the binding site. From the beginning to approximately 20 ns, lower Rg values of Na⁺-K⁺ ATPase in these complexes were observed compared with the protein itself, suggesting that the protein tightness was increased and the structure was changed into a tense

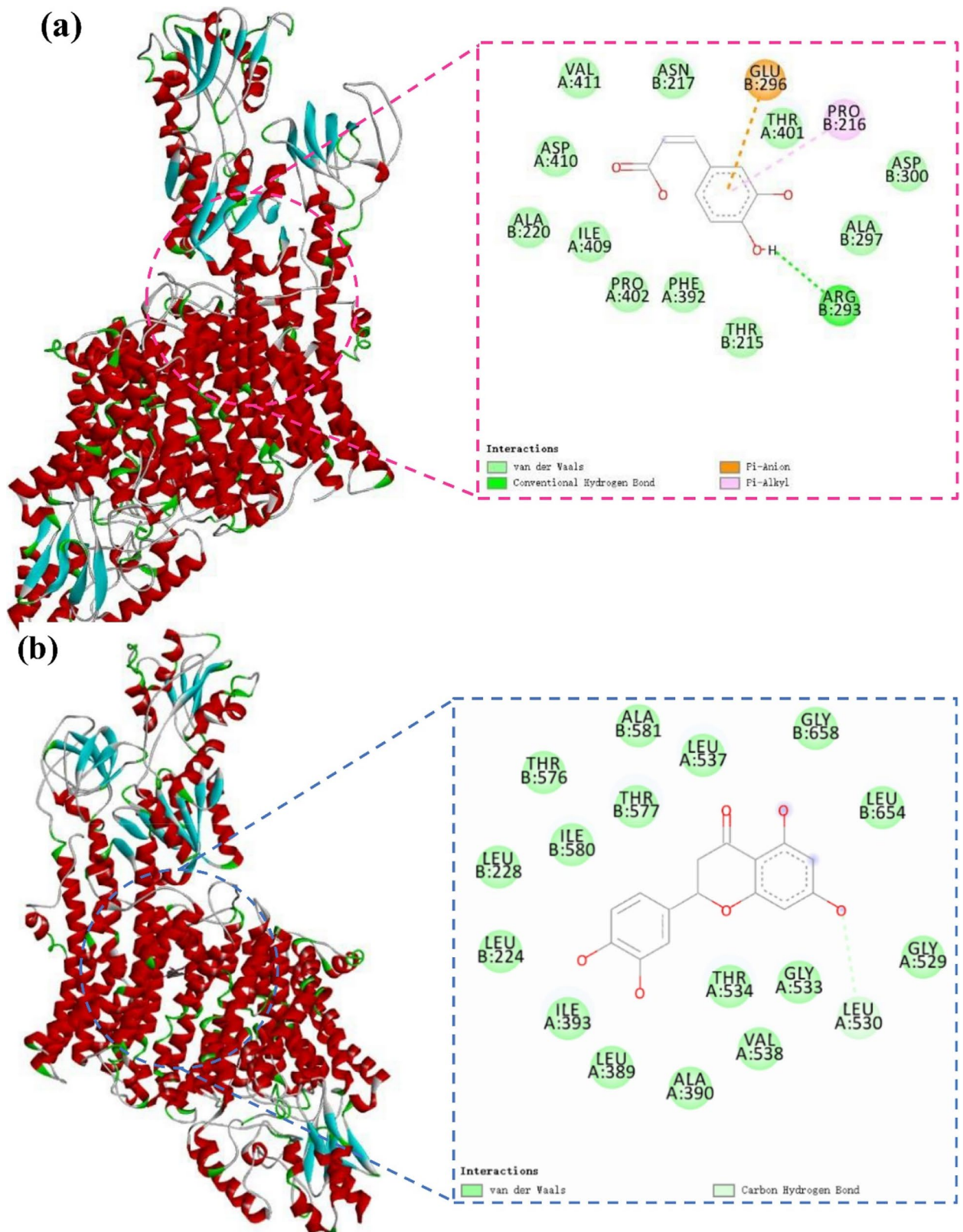


Fig. 5 The key representative phenols in dandelion extract docked with $\text{Na}^+\text{-K}^+$ ATPase of *E. coli*: **a** caffeic acid binding with the ATPase; **b** luteolin binding with the ATPase

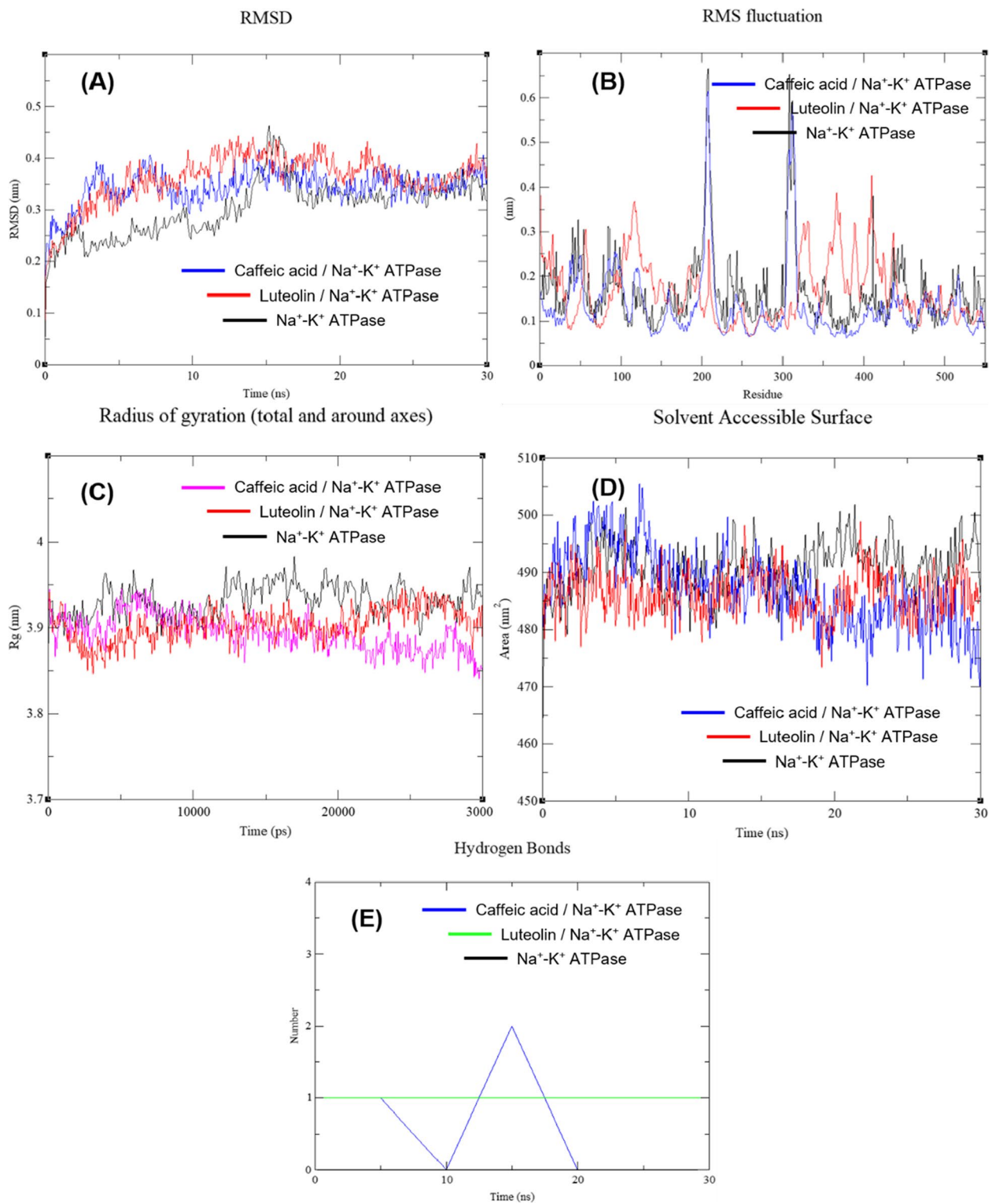


Fig. 6 The vital parameters such as RMSD (A), RMSF (B), Rg (C), SASA (D) and hydrogen numbers (E), derived from native protein (Na⁺-K⁺ ATPase), caffeic acid-protein complex and luteolin-protein complex in the process of MD; root mean square deviation (RMSD), root mean square fluctuation (RMSF), radius of gyration (Rg), hydrogen bond, solvent accessible surface area (SASA)

state when it was bonded with caffeic acid, in contrast to binding with luteolin. These results may be due to the insertion of caffeic acid / luteolin into the interior of the protein. As shown in Fig. 6C, the average Rg value of the caffeic acid/Na⁺-K⁺ ATPase complex systems was lower than that of luteolin / Na⁺-K⁺ ATPase, suggesting that fastening on the surface pressed the protein tighter with an increase in simulation time. We also found that the Rg value of the protein caused by caffeic acid was lower than that caused by luteolin, indicating a tighter protein structure resulting from caffeic acid. To further reveal the variation in the radius of gyration, the SASA values of the caffeic acid-binding Na⁺-K⁺ ATPase were monitored (Fig. 6D). The solvent-accessible surface, containing both hydrophobic and hydrophilic types, increased when the complex was formed, implying that the solvent over the surface of the peptides was improved, as well as the tighter and more compact structure of the protein. Likewise, over time, especially after 20 ns, the protein interacting with caffeic acid for closer binding affected the conformation of aromatic amino acids. The liganded protein became tighter owing to a lower SASA value.

Additionally, hydrogen bonding is a typical intermolecular weak interaction that is favorable for maintaining a compact and appropriate structure. Figure 6E shows the time dependence of the number of hydrogen bonds between Na⁺-K⁺ ATPase and caffeic acid or luteolin. The protein complex with caffeic acid reached two hydrogen bonds at 15 ns, whereas the protein complex with luteolin retained one hydrogen bond throughout the simulation period. These hydrogen bond formations between the protein and ligand are beneficial for forming a powerful and stable combination.

Overall, this study explored the antimicrobial function and mechanism of dandelion extracts from various organs (flowers, stems, leaves, and roots) against *E. coli*, which is beneficial for its efficient valorization and wide application. The identification results showed that caffeic acid and luteolin were predominant in all dandelion phenolic extracts. Dandelion flower phenolic extract (DFPE) was screened out of all the extracts because it had the highest level of total polyphenols, including caffeic acid and luteolin, and the strongest inhibition against *E. coli*. The inhibition of MIC and MBC for DFPE against *E. coli* reached 0.5 mg / mL and 1.0 mg / mL, respectively. In addition, an insightful antimicrobial mechanism in terms of cellular membrane leakage and ATPase activity inhibition was confirmed by monitoring the intracellular substance release level, extracellular ATP level, and Na⁺-K⁺ ATPase activity. Extensively increased levels of intracellular substances and extracellular ATP, as well as a

considerably decreased level of ATPase activity, were observed. Moreover, the docking results indicated that non-covalent forces, such as conventional hydrogen bonds, van der Waals forces, carbon hydrogen bonds, pi-alkyl, and pi-anion, were involved in the interactions between caffeic acid and ATPase in the cell membrane. Detailed results of the molecular dynamics showed that the complex structure of the protein reached equilibrium after 20 ns. The protein structure variation in the complex caused by caffeic acid binding became tighter and more compact by monitoring the lower values of key parameters (Rg, SASA, etc.), compared with the native protein itself. This highlighted new insights into the antibacterial function and mechanism of dandelion phenolic extracts against *Escherichia coli*.

Abbreviations

DFPE	Dandelion Flower Phenolic Extract
MIC	Minimum Inhibitory Concentration
MBC	Minimum Bactericidal Concentration
SEM	Scanning Electron Microscopy
LSCM	Laser Scanning Confocal Microscopy
Na ⁺ -K ⁺ ATPase	Na ⁺ -K ⁺ Adenosine Triphosphatase

Acknowledgements

We thank all the assistants for their help in the completion of this study.

Authors' contributions

Xie Pujun, Wang Xiang, Huang Lixin, Deng Yejun and Zhang Caihong conceived, designed the experiments, analyzed the data and wrote the manuscript.

Funding

This work was supported by the National Natural Science Foundation of China [grant no. 32271820] and the Natural Science Foundation of Jiangsu Province [grant no. BK20181124].

Availability of data and materials

The data available in this study are available in Tables 1 and 2; Figs. 1, 2, 3, 4, 5, and 6.

Declarations

Ethics approval and consent to participate

This study did not involve human participants, personal data, or negative environmental impacts.

Consent for publication

Not applicable.

Competing interests

Xie Pujun declares no competing interests. Wang Xiang declares no competing interests. Huang Lixin declares no competing interests. Deng Yejun declares no competing interests. Zhang Caihong declares no competing interests.

Author details

¹Institute of Chemical Industry of Forest Products, Chinese Academy of Forestry, National Engineering Laboratory for Biomass Chemical Utilization, Key and Open Laboratory on Forest Chemical Engineering, National Forestry and Grassland Administration, Key Laboratory of Biomass Energy and Material, Number 16 Suojin Wucun, Xuanwu District, Nanjing City, Jiangsu Province 210042, People's Republic of China. ²Co-Innovation Center of Efficient Processing and Utilization of Forest Resources, Nanjing Forestry University, Nanjing 210037, China.

Received: 7 October 2023 Accepted: 6 March 2024
Published online: 02 October 2024

References

- Al-Hakkani, M. F. (2019). A rapid, developed and validated RP-HPLC method for determination. *SN Applied Sciences*, 1, 222. <https://doi.org/10.1007/s42452-019-0237-6>
- Augustin, E., Moś-Rompa, A., Skwarska, A., Witkowski, J. M., & Konopa, J. (2006). Induction of G2/M phase arrest and apoptosis of human leukemia cells by potent antitumor triazoloacridinone C-1305. *Biochemical Pharmacology*, 72(12), 1668–1679. <https://doi.org/10.1016/j.bcp.2006.07.035>
- Chakraborti, S., Rahaman, S. M., Alam, M. N., Mandal, A., Ghosh, B., Dey, K., & Chakraborti, T. (2016). Na⁺/K⁺-ATPase: a perspective. In S. Chakraborti & N. Dhalla (Eds.), *Regulation of membrane Na⁺-K⁺ ATPase. Advances in biochemistry in health and disease*, vol 15. Cham: Springer. https://doi.org/10.1007/978-3-319-24750-2_1
- Dai, J., Li, C., Cui, H., & Lin, L. (2021). Unraveling the anti-bacterial mechanism of *Litsea cubeba* essential oil against *E. coli* O157:H7 and its application in vegetable juices. *International Journal of Food Microbiology*, 338, 108989. <https://doi.org/10.1016/j.ijfoodmicro.2020.108989>
- Di Pasqua, R., Hoskins, N., Betts, G., & Mauriello, G. (2006). Changes in membrane fatty acids composition of microbial cells induced by addition of thymol, carvacrol, limonene, cinnamaldehyde, and eugenol in the growing media. *Journal of Agricultural and Food Chemistry*, 54(7), 2745–2749. <https://doi.org/10.1021/jf052722l>
- Fedosova, N. U., Habeck, M., & Nissen, P. (2021). Structure and function of Na, K-ATPase-the sodium-potassium pump. *Comprehensive Physiology*, 12(1), 2659–2679. <https://doi.org/10.1002/cphy.c200018>
- Guo, L., Sun, Q., Gong, S. Y., Bi, X., Jiang, W., Xue, W., & Fei, P. (2019). Antimicrobial activity and action approach of the olive oil polyphenol extract against *Listeria monocytogenes*. *Frontiers Microbiology*, 10, 1586. <https://doi.org/10.3389/fmicb.2019.01586>
- Hu, C. (2018). Taraxacum: Phytochemistry and health benefits. *Chinese Herbal Medicines*, 10(4), 353–361. <https://doi.org/10.1016/j.jep.2016.02.050>
- Jedrejek, D., Kontek, B., Lis, B., Stochmal, A., & Olas, B. (2017). Evaluation of antioxidant activity of phenolic fractions from the leaves and petals of dandelion in human plasma treated with H₂O₂ and H₂O₂/Fe. *Chemico-Biological Interactions*, 262, 29–37. <https://doi.org/10.1016/j.cbi.2016.12.003>
- Kenny, O., Brunton, N. P., Walsh, D., Hewage, C. M., McLoughlin, P., & Smyth, T. J. (2015). Characterisation of antimicrobial extracts from dandelion root (*Taraxacum officinale*) using LC-SPE-NMR. *Phytotherapy Research*, 29(4), 526–532. <https://doi.org/10.1002/ptr.5276>
- Kolton, A., Długosz-Grochowska, O., Wojciechowska, R., & Czaja, M. (2022). Biosynthesis regulation of folates and phenols in plants. *Scientia Horticulturae*, 291, 110561. <https://doi.org/10.1016/j.scienta.2021.110561>
- Kou, J. C. (1957). The influence of some cations on an adenosine triphosphatase from peripheral nerves. *Biochimica et Biophysica Acta*, 23(2), 394–401. [https://doi.org/10.1016/0006-3002\(57\)90343-8](https://doi.org/10.1016/0006-3002(57)90343-8)
- Li, Y. N., Chen, Y. L., & Sun-Waterhouse, D. (2022). The potential of dandelion in the fight against gastrointestinal diseases: A review. *Journal of Ethnopharmacology*, 293, 115272. <https://doi.org/10.1016/j.jep.2022.115272>
- Lopez-Garcia, J., Kucekova, Z., Humpolicek, P., Mlcek, J., & Saha, P. (2013). Polyphenolic extracts of edible flowers incorporated onto atelocollagen matrices and their effect on cell viability. *Molecules*, 18(11), 13435–13445. <https://doi.org/10.3390/molecules181113435>
- Lu, Y. C., Zhao, R., Wang, C., Zhang, X. G., & Wang, C. A. (2022). Deciphering the non-covalent binding patterns of three whey proteins with rosmarinic acid by multi-spectroscopic, molecular docking and molecular dynamics simulation approaches. *Food Hydrocolloids*, 132, 107895. <https://doi.org/10.1016/j.foodhyd.2022.107895>
- Manges, A. R., Geum, H. M., Guo, A., Edens, T. J., Fibke, C. D., & Pitout, J. D. D. (2019). Global extraintestinal pathogenic *Escherichia coli* (ExPEC) Lineages. *Clinical Microbiology Reviews*, 32(3), e00135–e218. <https://doi.org/10.1128/CMR.00135-18>
- Minutolo, M., Amalfitano, C., Evidente, A., Frusciantè, L., & Errico, A. (2013). Polyphenol distribution in plant organs of tomato introgression lines. *Natural Product Research*, 27(9), 787–795. <https://doi.org/10.1080/14786419.2012.704371>
- Morones, J. R., Elechiguerra, J. L., Camacho, A., Holt, K., Kouri, J. B., Ramirez, J. T., & Yacaman, M. J. (2005). The bactericidal effect of silver nanoparticles. *Nanotechnology*, 16(10), 2346–2353. <https://doi.org/10.1088/0957-4484/16/10/059>
- Munoz, M. D., Plaza, A., Galan, A., Vicente, J. A., Martinez, M. P., & Acero, N. (2015). The effect of five *Taraxacum* species on in vitro and in vivo antioxidant and antiproliferative activity. *Food Function*, 6(8), 2787–2793. <https://doi.org/10.1039/c5fo00645g>
- Ochiai, H., Takeda, K., Soeda, S., Tahara, Y., Takenaka, H., Abe, K., Hayashi, Y., Noguchi, S., Inoue, M., Schwarz, S., Schwarz, W., & Kawamura, M. (2009). Epigallocatechin-3-gallate is an inhibitor of Na⁺, K⁽⁺⁾-ATPase by favoring the E1 conformation. *Biochemical Pharmacology*, 78(8), 1069–1074. <https://doi.org/10.1016/j.bcp.2009.06.007>
- Pinto, E., Vale-Silva, L., Cavaleiro, C., & Salgueiro, L. (2009). Antifungal activity of the clove essential oil from *Syzygium aromaticum* on *Candida*, *Aspergillus* and dermatophyte species. *Journal of Medical Microbiology*, 58(11), 1454–1462. <https://doi.org/10.1099/jmm.0.010538-0>
- Pivovarov, A. S., Calahorra, F., & Walker, R. J. (2018). Na⁺/K⁺-pump and neurotransmitter membrane receptors. *Invertebrate Neurosciences*, 19(1), 1–16. <https://doi.org/10.1007/s10158-018-0221-7>
- Poolman, J. T., & Anderson, A. S. (2018). *Escherichia coli* and *Staphylococcus aureus*: Leading bacterial pathogens of healthcare associated infections and bacteremia in older-age populations. *Expert Review of Vaccines*, 17(7), 607–618. <https://doi.org/10.1080/14760584.2018.1488590>
- Qi, Z. W., Xue, X. Y., Zhou, H., Yuan, H., Li, W. J., Yang, G. L., Xie, P. J., & Wang, C. Z. (2022). The aqueous assembly preparation of OPs-AgNPs with phenols from olive mill wastewater and its mechanism on antimicrobial function study. *Food Chemistry*, 376, 131924. <https://doi.org/10.1016/j.foodchem.2021.131924>
- Sengul, M., Yildiz, H., Gungor, N., Cetin, B., Eser, Z., & Ercisli, S. (2009). Total phenolic content, antioxidant and antimicrobial activities of some medicinal plants. *Pakistan Journal of Pharmacy*, 22(1), 102–106.
- Shi, R., Liu, Y., Ma, Y., Li, J., Zhang, W., Jiang, Z., & Hou, J. (2021). Insight into binding behavior, structure, and foam properties of α-lactalbumin/glycyrrhizic acid complex in an acidic environment. *Food Hydrocolloids*, 125, 107411. <https://doi.org/10.1016/j.foodhyd.2021.107411>
- Wang, L., Liu, L., Liu, Y., Wang, F., & Zhou, X. (2022). Antimicrobial performance of novel glutathione-conjugated silver nanoclusters (GSH@AgNCs) against *Escherichia coli* and *Staphylococcus aureus* by membrane-damage and biofilm-inhibition mechanisms. *Food Research International*, 160, 111680. <https://doi.org/10.1016/j.foodres.2022.111680>
- Wongsa, P., Phatiklungsun, P., & Prathumthong, S. (2022). FT-IR characteristics, phenolic profiles and inhibitory potential against digestive enzymes of 25 herbal infusions. *Scientific Reports*, 12(1), 6631. <https://doi.org/10.1038/s41598-022-10669-z>
- Xie, P. J., Huang, L. X., Zhang, C. H., Ding, S. S., Deng, Y. J., & Wang, X. J. (2018). Skin-care effects of dandelion leaf extract and stem extract: Antioxidant properties, tyrosinase inhibitory and molecular docking simulations. *Industrial Crops and Products*, 111, 238–246. <https://doi.org/10.1016/j.indcrop.2017.10.017>
- Xie, Z., & Askari, A. (2002). Na⁺/K⁺-ATPase as a signal transducer. *European Journal of Biochemistry*, 269(10), 2434–2439. <https://doi.org/10.1046/j.1432-1033.2002.02910.x>
- Xu, P., Xu, X. B., Khan, A., Fotina, T., & Wang, S. H. (2021). Antibiofilm activity against *Staphylococcus aureus* and content analysis of *Taraxacum Officinale* phenolic extract. *Polish Journal of Veterinary Sciences*, 24(2), 243–251. <https://doi.org/10.24425/pjvs.2021.137659>
- Zhao, L., Zhang, H. Y., Hao, T. Y., & Li, S. R. (2015). In vitro antibacterial activities and mechanism of sugar fatty acid esters against five food-related bacteria. *Food Chemistry*, 187, 370–377. <https://doi.org/10.1016/j.foodchem.2015.04.108>
- Zhou, Y., Yao, Q. F., Zhang, T., Chen, X. Q., Wu, Z. Q., Zhang, N., Shao, Y. D., & Cheng, Y. (2020). Antibacterial activity and mechanism of green tea polysaccharide conjugates against *Escherichia coli*. *Industrial Crops and Products*, 152, 112464. <https://doi.org/10.1016/j.indcrop.2020.112464>

Publisher's Note

Springer Nature remains neutral with regard to jurisdictional claims in published maps and institutional affiliations.